

Session 6
General Topics

A cellular automaton model for coronal heating

M. C. López Fuentes^{1,2} and J. A. Klimchuk³

¹Instituto de Astronomía y Física del Espacio (CONICET-UBA), CC 67, Suc 28,
1428 Buenos Aires, Argentina
email: lopezf@iafe.uba.ar

²Facultad de Cs. Exactas y Naturales, Universidad de Buenos Aires, Argentina

³NASA Goddard Space Flight Center, Code 671, Greenbelt, MD 20771, USA

Abstract. We present a simple coronal heating model based on a cellular automaton approach. Following Parker's suggestion (1988), we consider the corona to be made up of elemental magnetic strands that accumulate magnetic stress due to the photospheric displacements of their footpoints. Magnetic energy is eventually released in small scale reconnection events. The model consists of a 2D grid in which strand footpoints travel with random displacements simulating convective motions. Each time two strands interact, a critical condition is tested (as in self-organized critical models), and if the condition is fulfilled, the strands reconnect and energy is released. We model the plasma response to the heating events and obtain synthetic observations. We compare the output of the model with real observations from Hinode/XRT and discuss the implications of our results for coronal heating.

Keywords. Sun: corona, Sun: magnetic fields, Sun: activity

1. Introduction

Research works in recent years strongly suggest that the basic constituents of the coronal magnetic structure are unresolved elementary strands rooted in the photosphere (Reale 2010). In the late 80's, Parker (1988) proposed a scenario for coronal heating based on the continual dragging of strand footpoints by photospheric convection. In this scheme, footpoint motions tangle adjacent strands, producing magnetic stress between them and creating favorable conditions for reconnection and energy release. The actual reconnection events occur when neighboring strands reach a critical misalignment. Dahlburg *et al.* (2005) proposed the Secondary instability as a possible a mechanism for such critical release.

The process described above was explored in a wide variety of studies ranging from nanoflare heating models for coronal loop dynamics (see e.g., Cargill & Klimchuk 2004) to self-organized criticality in relation to flare energy power-law distributions (see e.g., Morales & Charbonneau 2008). We recently developed a simple cellular automaton (CA) model based on the above ideas (López Fuentes & Klimchuk 2010) to explain the intensity evolution of Soft X-ray loops. Here, we present a more sophisticated 2D approach. We use our model to construct synthetic light curves and compare them with observations obtained with the X-ray Telescope (XRT) on board Hinode.

2. Description of the model

The model consists of a square grid of sites initially occupied by a uniform distribution of movable points that we associate with magnetic strands (see Figure 1, panel a). At each

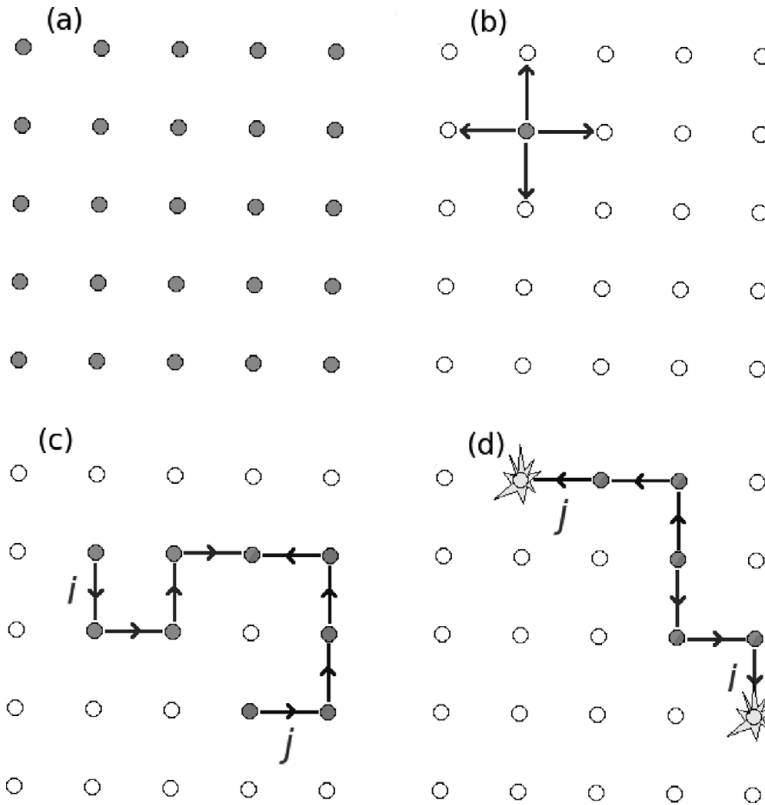


Figure 1. Scheme of the CA model described in Section 2.

time step, the points move to random neighbor positions, one site at a time, simulating photospheric displacements (Figure 1, panel b). Assuming that in the initial distribution all strands are parallel and untangled (panel a), as the system evolves the horizontal magnetic field components of the strands increase. As fully explained in López Fuentes & Klimchuk (2010), the magnitude of the increase in each time step is approximately given by:

$$\delta B_h = B_v d/L, \quad (2.1)$$

where B_v is the vertical component of the magnetic field, L is the strand length and d is a typical length of a photospheric displacement. Here, we consider $d = 1000$ km, corresponding to the approximate distance travelled by a strand footpoint during a convective cell turnover time. Defining S_i as the number of steps travelled by strand i , it is easy to see that, as time goes on, the horizontal component of the field becomes $\approx S_i \delta B_h$. As the system continues evolving, the “strand-points” travel through the grid increasing their paths and their horizontal field components. Whenever two strands (identified with indices i and j in Figure 1, panel c) occupy the same grid position, we consider them to become linked. Strands i and j continue travelling separately but the link is kept (see Figure 1, panel d). We define the critical magnetic field: $B_c = B_v \tan \theta_c$. When the field associated with the mutual displacement of the linked strands surpasses B_c according to:

$$\Delta B = \frac{B_v d}{L} (S_i + S_j) > B_c, \quad (2.2)$$

(i.e., when the misalignment angle exceeds the critical value θ_c), then the strands

reconnect and magnetic energy is released. After that, the strands become unlinked and their horizontal field components are diminished in a consistent manner. It can be easily shown that each of these reconnection events (or nanoflares) releases:

$$E_{ij} = \frac{B_v^2 d^2}{8\pi L^2} [(S_i'^2 + S_j'^2) - (S_i^2 + S_j^2)], \quad (2.3)$$

where:

$$S_i' = \alpha(S_i - 1) + (1 - \alpha)(S_j - 1), \quad (2.4)$$

$$S_j' = (1 - \alpha)(S_i - 1) + \alpha(S_j - 1), \quad (2.5)$$

and α is a random parameter ($0 < \alpha < 1$) that accounts for the fact that reconnection between strands is not necessarily symmetrical (the relative lengths of the old and new strands may change).

The output of the model is the set of nanoflares that occurred in each strand after all of the footpoints in the system have been displaced. The nanoflares are modeled as triangular heating functions. To simulate the response of the plasma to the heating we use the EBTEL model (Enthalpy-Based Thermal Evolution of Loops, see Klimchuk *et al.* 2008). Using the known XRT response and the plasma density and temperature output from EBTEL, we obtain the expected emission observed with the XRT instrument. We add the contribution of all strands to the emission and correct for the number of strands covered by a single pixel. We also model the photon noise by adding intensity fluctuations using a Poisson distribution with the amplitude provided by Narukage *et al.* (2011).

3. Comparison with observations

We compare synthetic light curves obtained in this manner with Hinode/XRT observations. The analyzed data were obtained with the Al_Kpoly filter, and correspond to NOAA AR 11147, observed on January 18, 2011. The time span of the data is approximately 8000 sec with a cadence of ~ 10 sec. The images were processed and coaligned using Solar Software routines. In Figure 2, upper panels, we show the light curves of two of the loops selected from the dataset. The lower panels correspond to portions of model light curves with the same durations. For the models we use the following typical solar parameters: $B_v = 100$ G, $L = 100$ Mm, $\tan \theta_c = 0.25$, $N = 121$ (number of strands) and $\tau = 200$ sec (nanoflare duration).

Obviously, given the random nature of the model, it is not reasonable to expect a one to one correspondence between synthetic and observed light curves. For the comparison we rather consider general properties such as mean intensities and standard deviations. This kind of analysis shows that both observed and synthetic light curves in Figure 2 have a mean intensity of ~ 2400 DN/pix and a standard deviation of ~ 300 DN/pix, which is around 12% of the signal.

It is worth noting that part of the observed fluctuations is due to photon noise. However, the photon noise contribution has a smaller amplitude and a shorter characteristic timescale than the longer term fluctuations that produce most of the measured intensity standard deviation. To characterize the short term variation we compute the *rms* of the intensity with respect to the 10-point running average. Both observations and model have a relative *rms* of 0.04. This supports our modeling of the photon noise and suggests that longer term fluctuations are intrinsic, and are due to the variation of the individual strand intensities.

In a recent paper, Terzo *et al.* (2011) found in Hinode/XRT observations a difference between the mean and the median values of intensity fluctuation distributions. They

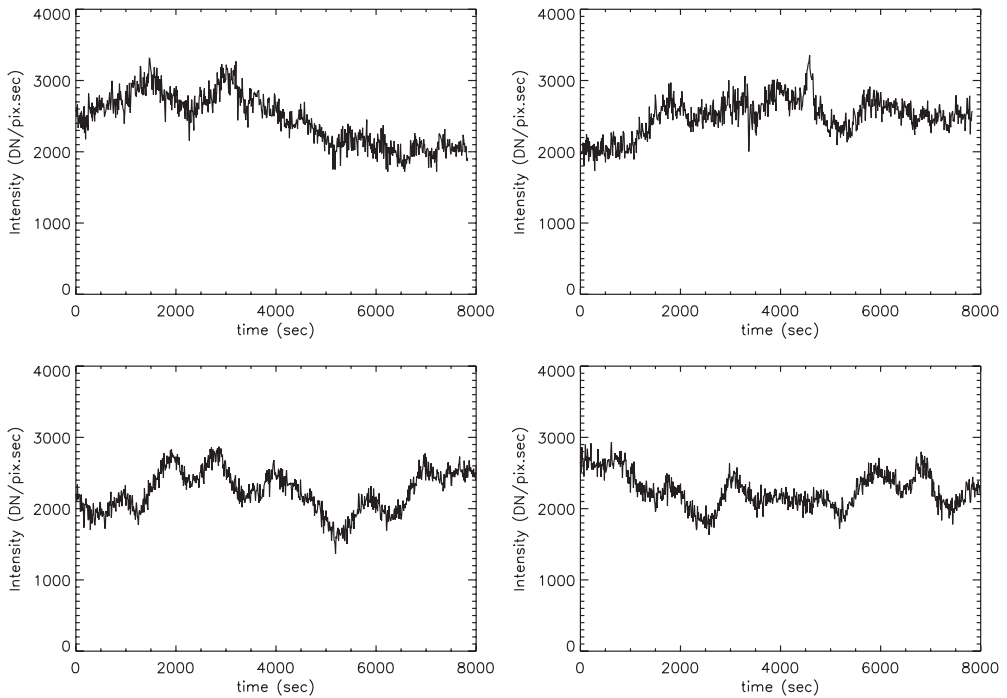


Figure 2. Upper panels: Loop light curves obtained from Hinode/XRT observations. Lower panels: Synthetic light curves obtained with the CA model presented in Section 2.

interpreted this as a signature of nanoflare heating. We not only confirm their findings in the loops studied here, but we also find the same differences between the mean and median values in the model light curves. These are very interesting results and we plan to continue exploring their implications in the near future.

4. Conclusions

We developed a CA model that reproduces the basic characteristics of Hinode/XRT loop light curves. The first results are encouraging. Among future investigations, we plan to explore the full space of parameters of the model to obtain scaling laws of the light curve properties with these parameters. We will also include in our analysis SDO/AIA observations to study how the model compares with the evolution of EUV loops.

References

- Cargill, P. J. & Klimchuk, J. A. 2004, *Astrophys. J.*, 605, 911
 Dahlburg, R. B., Klimchuk, J. A., & Antiochos, S. K. 2005, *Astrophys. J.*, 622, 1191
 Klimchuk, J. A., Patsourakos, S., & Cargill, P. J. 2008, *Astrophys. J.*, 682, 1351
 López Fuentes, M. C. & Klimchuk, J. A. 2010, *Astrophys. J.*, 719, 591
 Morales, L. & Charbonneau, P. 2008, *Astrophys. J.*, 682, 654
 Narukage, N., Sakao, T., Kano, R., *et al.* 2011, *Sol. Phys.*, 269, 169
 Parker, E. N. 1988, *Astrophys. J.*, 330, 474
 Reale, F. 2010, *Living Reviews in Solar Physics*, 7, 5
 Terzo, S., Reale, F., Miceli, M., *et al.* 2011, *Astrophys. J.*, 736, 111